THE JOURNAL OF PHYSICAL CHEMISTRY B

ARTICLE

pubs.acs.org/JPCB

Scattering Density Profile Model of POPG Bilayers As Determined by Molecular Dynamics Simulations and Small-Angle Neutron and X-ray Scattering Experiments

Norbert Kučerka,[*,†,‡] Bryan W. Holland,[§] Chris G. Gray,[§] Bruno Tomberli,[∥] and John Katsaras[*,†,§,⊥,¶,#]

[†]Canadian Neutron Beam Centre, National Research Council, Chalk River, Ontario K0J 1J0, Canada

[‡]Department of Physical Chemistry of Drugs, Faculty of Pharmacy, Comenius University, 832 32 Bratislava, Slovakia

[§]Department of Physics and Biophysics Interdepartmental Group, University of Guelph, Guelph, Ontario N1G 2W1, Canada

[∥]Department of Physics and Astronomy, Brandon University, Brandon, Manitoba R7A 6A9, Canada

[⊥]Department of Physics, The University of Tennessee, Knoxville, Tennessee 37996-1200, United States

[¶]Biology and Soft Matter Division, Neutron Sciences Directorate, Oak Ridge National Laboratory, Oak Ridge, Tennessee 37831-6100, United States

[#]Joint Institute for Neutron Sciences, Oak Ridge National Laboratory, Oak Ridge, Tennessee 37831-6453, United States

ABSTRACT: We combine molecular dynamics (MD) simulations and experiment, both small-angle neutron (SANS) and small-angle X-ray scattering (SAXS), to determine the precise structure of bilayers composed of 1-palmitoyl-2-oleoyl-*sn*-glycero-3-phosphatidylglycerol (POPG), a lipid commonly encountered in bacterial membranes. Experiment and simulation are used to develop a one-dimensional scattering density profile (SDP) model suitable for the analysis of experimental data. The joint refinement of such data (i.e., SANS and SAXS) results in the area per lipid that is then used in the fixed-area simulations. In the final step, the direct comparison of simulated-to-experimental data gives rise to the detailed structure of POPG bilayers. From these studies we conclude that POPG's molecular area is 66.0 ± 1.3 Å^2, its overall bilayer thickness is 36.7 ± 0.7 Å, and its hydrocarbon region thickness is 27.9 ± 0.6 Å, assuming a simulated value of 1203 Å^3 for the total lipid volume.

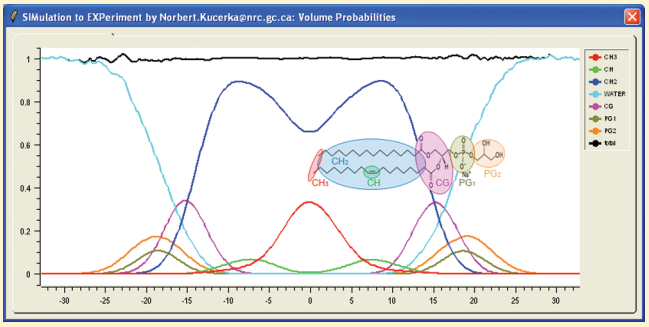

INTRODUCTION

The complex dynamics exhibited by biological membranes—a common characteristic of amphiphilic systems—are closely correlated with the membrane's overall structure. It should therefore not come as a surprise that accurate structural data regarding the various membrane components (e.g., area per lipid, bilayer thickness, etc.) are important in determining specific biomembrane functions. For example, recent studies suggest that certain peptides are capable of compromising certain bacterial membranes, and may therefore have the potential to either replace or augment traditionally used antibiotics.[1] The design of new and more effective peptides, however, requires a deeper understanding of when and how specificity occurs.

The binding free energy, for example, of lactoferricin B to mammalian-like membranes (i.e., neutral membranes, e.g., 1-palmitoyl-2-oleoyl-*sn*-glycero-3-phosphatidylcholine, POPC) and bacterial-like membranes (i.e., net negative charge membranes, e.g., 1-palmitoyl-2-oleoyl-*sn*-glycero-3-phosphatidylglycerol, POPG) has been predicted from molecular dynamics (MD) simulations.[2,3] However, for the simulation to make any kind of prediction, an accurate structure of the lipids making up the membrane is needed. When such a structure is not available, as is usually the case, the atom−atom potential interaction parameters producing the inputted lipid structure can be "tweaked" to improve the fit between simulated and experimental data. One quantity that is often adjusted is a lipid's lateral area, which is commonly understood to influence lipid−lipid and lipid−peptide interactions, and which plays a central role in the outcome of MD simulations. In the case of POPC, and other neutral membranes, the area per lipid is known from both simulation and experiment.[4] However, for POPG, and other charged lipid bilayers, experimental values have yet to be determined. Importantly, the values from simulation using the standard CHARMM and GROMACS force fields disagree with each other.[3,5] Thus, experimental data for POPG, and other commonly used lipids, are necessary to resolve the discrepancy between the two main simulation approaches, and to guide modeling approaches that more accurately describe biomimetic membrane systems.

X-ray and neutron scattering are arguably two of the most powerful experimental techniques when it comes to elucidating

Received: September 15, 2011
Revised: November 21, 2011
Published: November 22, 2011

dx.doi.org/10.1021/jp208920h | *J. Phys. Chem. B* 2012, 116, 232–239

the structure of biomembranes.[6] At the same time, the two techniques complement each other as they are differentially sensitive to different parts of the lipid bilayer. For example, in the case of X-rays the electron-dense (ED) phosphate groups contrast very well with the lower electron density hydrocarbon region. Thus, X-ray data are well suited for the refinement of lipid headgroups and hydrocarbon chains. On the other hand, the high neutron scattering length density (NSLD) of D_2O (often used in neutron experiments instead of H_2O) permits neutron scattering experiments to accurately determine the total bilayer thickness and, consequently, lipid area when volumetric information is available.[7] In order to address this complementarity, we recently developed a model for calculating scattering density profiles (SDP)[7] whereby the data sets from the two techniques are jointly refined - an approach pioneered by Wiener and White.[8] Thus, by appropriately parsing a lipid molecule and simultaneously analyzing the different experimentally obtained "contrast" data (i.e., X-ray and different deuteration neutron scattering data), a more precise structure of the bilayer can be determined.

Area per lipid is often used as the key parameter when assessing the validity of MD simulations. However, similar to the disparate experimentally obtained results for lipid areas, published MD simulations have also reported a wide range of values. For example, CHARMM (Chemistry at HARvard Molecular Mechanics) force field based simulations show a dramatic lateral condensation and overly ordered lipid acyl chains,[9] which in the case of DPPC (1,2-dipalmitoyl-*sn*-glycero-3-phosphatidylcholine) bilayers do not resemble the experimentally observed fluid phase structure.[10] This simulation pitfall can, however, be avoided by applying an appropriate positive surface tension,[11,12] which requires the use of precise areas per lipid. Another attempt to enhance the predictive power of MD simulations assigns new partial charges to the lipid's headgroup and upper acyl chains, the so-called CMAP correction.[13] Although focused on DPPC, even this approach underestimates the fluid phase area per DPPC molecule by about 4 Å^2. In contrast, OPLS (Optimized Potential for Liquid Simulations) based force fields do not seem to require this additional tweaking.[14] The same level of lateral condensation is not observed in DOPC (1,2-dioleoyl-*sn*-glycero-3-phosphatidylcholine) bilayers, possibly due to the different melting temperatures inherent to the two bilayer systems (i.e., DPPC and DOPC).[15] It is also known, both from experiment and from simulation, that the number of double bonds and their positions within the lipid's acyl chains have a pronounced effect on area per lipid.[16] Finally, there is another layer of complexity in determining areas per lipid in bilayers with a net charge (e.g., such as the PG bilayers studied here), that of additional electrostatic interactions.

Given this situation, many simulations have opted to fix the area per lipid to experimentally obtained values. On the other hand, lipid areas obtained from experiment have also used models that were guided by simulation data, and are thus also model dependent. It has therefore been proposed that a better test for validating MD simulations is to compare them to "raw" experimental data (e.g., scattering form factors).[17,18] Experimentally obtained scattering form factors then become the basis for the synergy between experiment and simulation, whereby simulation results guide the development of more realistic models, and in turn, experimentally obtained data aid in the development of more accurate MD force fields.

We employ the above-described approach to determine the structural parameters of bilayers made of POPG. MD simulations are initiated at a fixed area per lipid of 62.9 Å^2 and compared directly to the unrefined experimental data obtained from SAXS and SANS measurements. The simulation-to-experiment comparison using the SIMtoEXP software[19] reveals significant differences between the two, thus requiring a further iteration of the simulations. Nevertheless, the original simulations provide useful information that guide the model's development into one that is suitable for the analysis of experimental data. The derived SDP model for POPG is then simultaneously fitted to SAXS and different contrast SANS data (i.e., different levels of deuteration), with a resultant area per lipid of 66.0 Å^2. Finally, MD simulations are performed at the experimentally determined area and are compared to raw experimental data. Agreement between experiment and simulation confirms the area per lipid value, with simulation providing further information regarding structural details of POPG bilayers.

MATERIALS AND METHODS

Synthetic 1-palmitoyl-2-oleoyl-*sn*-glycero-3-phosphatidylglycerol (C16:0-18:1PG, POPG) was purchased from Avanti Polar Lipids (Alabaster, AL) and used without further purification. Fifty milligrams of POPG was mixed with 1 mL of 100 mM NaCl solution made using D_2O (99.9% pure, Chalk River Laboratories), while 7.5 mg of POPG was mixed with 0.4 mL of nondeuterated 100 mM NaCl solution (18 MΩcm H_2O). Lipid mixtures were temperature cycled through the main phase transition until uniform dispersions of multilamellar vesicles (MLVs) were obtained. Unilamellar vesicles (ULVs) were then prepared from these dispersions at temperatures above POPG's main phase transition temperature (−2 °C)[20] using an Avanti mini-extruder fitted with two 0.25 mL airtight syringes. MLVs were extruded through two polycarbonate filters populated with 500 Å diameter pores, producing ULVs with diameters of ∼600 Å.[21] Finally, samples were diluted with D_2O or H_2O (100 mM NaCl solutions) to the desired external contrast condition (i.e., 100%, 70% and 50% D_2O in the case of neutron contrast variation experiments, and 100% H_2O in the case of X-ray scattering experiments). The total lipid concentration of all ULV samples was ∼20 mg/mL, guaranteeing the presence of sufficient amounts of water between ULVs, thus eliminating the possibility of interparticle interactions (i.e., structure factor).[21]

Small-Angle X-ray Scattering. X-ray data were taken at the G-1 station located at the Cornell High Energy Synchrotron Source (CHESS). A 1.18 Å wavelength (λ) X-ray beam of dimensions 0.24 × 0.24 mm^2 was detected using a 1024 × 1024 pixel array FLICAM charge-coupled device (CCD) with 71 μm linear dimension pixels. The sample-to-detector distance (SDD) was 423.6 mm, as determined using silver behenate (d-spacing of 58.367 Å). Samples were contained in 1.5 mm quartz capillaries placed in a temperature-controlled, multiple position sample holder. Two-dimensional (2D) images were dezingered using two consecutive 10 s exposures and corrected using calibration files supplied by CHESS. Data sets were normalized using the incident beam intensity as measured by an ion chamber. Background scattering resulting from water and air was subtracted according to the procedure described in ref 21. An additional linear function was used to correct for an unaccountable rise in background scattering, most likely due to an increase in the sample-to-detector path length at higher angles, while an absorption correction was found unnecessary.[4] Finally, the experimental scattering form factor moduli were obtained using

$$|F_e(q)| = \mathrm{sign}(I(q))\sqrt{|I(q)|q^2} \quad (1)$$

dx.doi.org/10.1021/jp208920h |*J. Phys. Chem. B* 2012, 116, 232–239

Note the possibility of some unphysical negative values for $|F_e(q)|$, the result of negative $I(q)$ values when $I(q)$ approaches zero. The statistical noise near zero values requires a distribution of amplitudes that unavoidably includes some negative values. It should be pointed out, however, that ignoring such negative values would unduly bias the end results.[22]

Small-Angle Neutron Scattering. Neutron scattering data were taken at the NG-7 station[23] located at the National Institute of Standards and Technology (NIST) Center for Neutron Research (NCNR). Six angstrom wavelength neutrons were selected using a mechanical velocity selector with the desired neutrons having an energy dispersion of 11.5% (fwhm). Multiple sample-to-detector distances (i.e., 2, 5, and 15.3 m) were used, resulting in a total scattering vector [$q = 4\pi/\lambda \sin(\theta)$, where λ is the wavelength and 2θ is the scattering angle] of $0.003 < q < 0.3$ Å^{-1}. Data were collected using a 2D ^{3}He position-sensitive detector with a 5 mm × 5 mm resolution (640 × 640 mm^2). Samples were taken up in standard 1 mm path length quartz cells. Collected 2D images were corrected and reduced into 1D scattering curves using software supplied by NIST,[24] while no additional absorption corrections were applied.[4] Scattering form factors were obtained using eq 1.

Molecular Dynamics Simulations. Molecular dynamics (MD) simulations were performed using NAMD 2.7[25] with the standard CHARMM 27 force field[26] (without the CMAP correction[13]) and the TIP3P water model. By default, this force field uses the Roux parametrization for ions,[27] rather than Aqvist parametrization[28] whose strong bonding in solution may lead to ionic crystallization.

The system consisted of 288 POPG lipids (144 per leaflet) and 9619 water molecules. Enough Na^+ was added to neutralize the negatively charged POPG molecules, and NaCl was added to create a 100 mM solution, mimicking both physiological and experimental conditions. The bilayer was created using the membrane building tools available on the CHARMM-GUI Web site,[29] and the remaining system was added using the software VMD.[30] Standard periodic boundary conditions were used to minimize boundary effects, and a constant particle number, area, normal pressure, and temperature (NAP_nT ensemble) were used to constrain the membrane such that the POPG area in the $x-y$ plane remained unaltered. The pressure normal to the bilayer was then held fixed, allowing the z-axis to expand and contract in order to achieve a constant P_n. A temperature of 298 K was used in order to replicate experimental conditions and was controlled using the Langevin dynamics based thermostat provided with NAMD. Rigid bonds were used for all hydrogen atoms, thus allowing a time step of 2 fs to be used; sampling was performed every picosecond to ensure a weak correlation between sample points.

The initial system maintained an area per lipid of 62.9 Å^2 and was equilibrated for 20 ns prior to 40 ns of production run time. From this production trajectory, probability distributions for each atom type in the lipid, $P_i(z)$, were created with $z = 0$ defining the geometric center of the bilayer. A second simulation was performed to confirm the experimental result by constraining the simulation area per lipid to 65.99 Å^2. The system was again equilibrated for 20 ns, but this time with the production portion running for 20 ns. From this condition, another set of $P_i(z)$ values were calculated and analyzed.

RESULTS AND DISCUSSION

MD simulations were first performed at the fixed area per lipid of 62.9 Å^2, a value based on literature data for similar lipids. A smaller area per lipid of 60.6 Å^2 was obtained in our initial simulation whereby the $x-y$ lateral plane was not constrained (i.e., NpT ensemble). However, it has been pointed out that such approaches result in a dramatic lateral contraction and in overly ordered lipid acyl chains.[9,13,31] Of note is that we do not use the simulation to provide accurate lipid areas, but as a way to guide the SDP model. Therefore, although the design of the SDP model is based on a simulation, when it comes to fitting experimental data, critical parameters such as lipid area, bilayer thickness, and the width of the probability distributions are not constrained. In other words, the model only assumes the functional forms of the probability distributions which are obtained from simulations and do not vary to any great extent with the detailed simulation. Our analysis, therefore, does not assume numerical values for those critical parameters that may be different for different lipid bilayers.

All atom simulations, such as the one employed here, provide complete probability distributions for the various atoms and can thus be used to calculate SDPs without any prior assumptions. SDPs are then easily transformed into q-space (i.e., reciprocal space) via the continuous Fourier transform[19] as follows:

$$|F_s(q_z)| = \left| \int_{-D/2}^{D/2} \left(\sum_\alpha f_\alpha(q_z) n_\alpha(z) - \rho_s \right) (\cos(zq_z)\, dz + i \sin(zq_z))\, dz \right| \quad (2)$$

where $n_\alpha(z)$ are the atomic number distributions obtained from simulation and ρ_s is the scattering density of the solvent, which is equal either to the solvent's (i.e., water) number of electrons (in the case of X-rays) or its neutron scattering length (in the case of neutrons) divided by its volume ($V_{WAT} = 29.0$ Å^3 as obtained from our simulation). In the case of neutron scattering, $f_\alpha(q_z)$ corresponds to the neutron scattering length b_α and does not depend on the scattering vector q_z as nuclei are effectively point sources for neutrons with wavelengths of the order of interatomic distances, while in the case of X-ray scattering, $f_\alpha(q_z)$ is the atomic form factor, which is given by the Fourier transform of the atomic electron density (see ref 19 for more details). Calculated scattering form factors are then readily available for comparison with unrefined experimental data.

Experimental scattering data consist of measured intensities that can easily be converted to form factors using eq 1.[22] While form factors calculated from simulations, $|F_s(q)|$, are on an absolute scale, experimental data are commonly only obtained on a relative scale. However, the scaling factor, k_e, for each independent set of experimental form factors, $|F_e(q)|$, is readily calculated from[32]

$$k_e = \frac{\sum_{i=1}^{N_q} \frac{|F_s(q_i)||F_e(q_i)|}{(\Delta F_e(q_i))^2}}{\sum_{i=1}^{N_q} \frac{|F_e(q_i)|^2}{(\Delta F_e(q_i))^2}} \quad (3)$$

where the summation goes through all of the experimental data (N_q), and where $\Delta F_e(q)$ is the experimental uncertainty of each datum. The overall agreement/disagreement between the simulation and the experimental data can be seen in the plots shown in

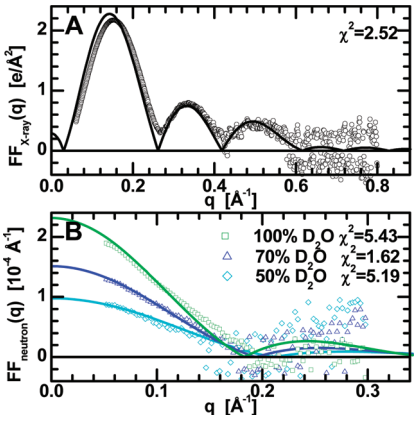

Figure 1. X-ray (A) and different neutron contrast scattering form factors (B) calculated from MD simulation data with A = 62.9 Å^2 (solid lines), and compared to experimental data (points). Experimental data are scaled according to eq 3, and χ^2 are calculated according to eq 4.

Figure 1, and/or it can be quantified via a reduced χ^2, which is calculated by the SIMtoEXP[19] program as

$$\chi^2 = \frac{\sqrt{\sum_{i=1}^{N_q} \left(|F_s(q_i)| - k_e|F_e(q_i)|\right)^2/\left(\Delta F_e(q_i)\right)^2}}{\sqrt{N_q - 1}} \qquad (4)$$

The simulation-to-experiment comparison shown in Figure 1 reveals significant differences between the two, indicating the need for further refinement. Although the MD simulation describes the X-ray data reasonably well in the range above $q \sim 0.2$ Å^{-1}, the χ^2 calculated for the neutron scattering data from experiment in 100% D_2O and simulation, suggests a larger area per lipid. From this comparison, however, it is not clear how to estimate the exact structural parameters values. In order to ameliorate the situation, one approach is to run several simulations with different values for A (equivalent to different surface tensions), and the simulation that best fits the experimental data then provides a model-free method for determining bilayer structure.[17] Clearly, this simulation-based approach is independent of structural models and can be used to determine the structural properties of different lipid bilayers, including those containing dopant molecules such as cholesterol or peptides. The initial simulation does, however, provide useful information for designing the model that can eventually be utilized in the model-based analysis of the experimental data, and thus results in guidelines for selecting values for A. Using this approach, the number of time-consuming MD simulations can be reduced to a minimum.

SDP Model for POPG. It has previously been shown that the SDP model of unsaturated hydrocarbon chains is best divided into terminal methyl (CH_3), methine (CH) and methylene (CH_2) groups,[7,8,33] a parsing scheme that we have adopted for our POPG model. However, the differences between PC and PG require us to re-evaluate the parsing of the headgroup. An obvious choice is to combine the carbonyl and glycerol atoms into one component (CG), as was the case for the PC SDP model.[7] However, the arrangement of atoms in the PG headgroup suggests separate components for the phosphate (PG1) and glycerol (PG2) groups (Figure 2).

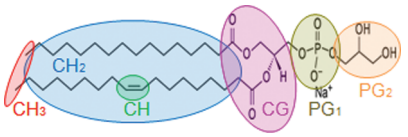

Figure 2. Schematic showing the SDP model parsing of POPG. Lipid chains are divided into terminal methyl (CH_3), methine (CH), and methylene (CH_2) groups, while the PG headgroup consists of carbonyl—glycerol (CG), phosphate (PG1) and glycerol (PG2) components.

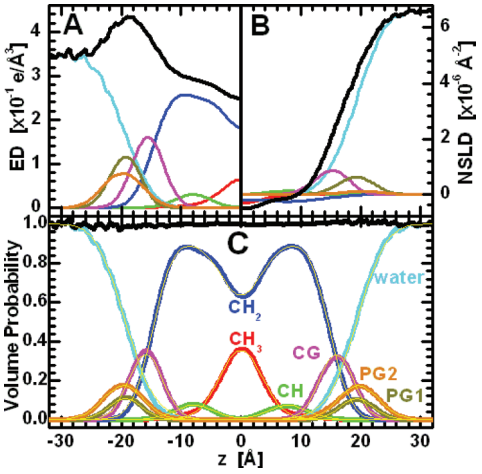

Figure 3. Electron densities (A) and neutron scattering length densities (B) of the different component distributions that comprise a POPG bilayer, including the total scattering density (thick black lines). The SDP model representation (thin lines) of the lipid bilayer applied to MD simulation data (thick lines) in terms of volume probability distributions is shown in panel C. Small fluctuations of the total probability (thick black line) taking place around 1 are an indication of a realistic parsing of the lipids components in the SDP model.

It has also been shown[7] that the combination of two Gaussians (one for CH_3 and one for CH components) along with the classical error function is suitable for describing the probabilities and scattering densities (i.e., ED and NSLD) of lipid hydrocarbon chains in the SDP model (see Figure 3). However, unlike the case of the PC headgroup, where a nonintuitive parsing had to be implemented in order to accommodate the negative NSLD of the choline, the choline-free PG headgroup has positive Gaussians for both PG1 and PG2 components (Figure 3), further making the case for the above-mentioned parsing scheme. Moreover, our MD simulation results suggest the overlap of these two components (i.e., PG1 and PG2), thus providing the option to simplify our model by combining the two Gaussians (i.e., PG1 and PG2) into one (i.e., PG). Nevertheless, we include both headgroup parsing scenarios in our analysis and propose that the use of a single PG Guassian is appropriate when the experimental data is not of high enough statistical quality - a situation that benefits through the use of a reduced number of model parameters. The data with regard to the PG1—PG2 vector, which in our case implies an orientation parallel to the bilayer surface, may prove important in providing a more detailed description of PG headgroup structure.

The SDP model of POPG (Figure 2) is simultaneously fitted to POPG SAXS and three contrast SANS (i.e., measured in 100, 70, and 50% D_2O) bilayer data collected at 30 °C. The four sets of experimental data that are used to fit a single set of model

dx.doi.org/10.1021/jp208920h |J. Phys. Chem. B 2012, 116, 232–239

Table 1. Structural Results Obtained from Using the SDP Model To Fit MD Simulated and Experimental Data of 30 °C POPG Bilayers[a]

	MD at 62.9 Å^2	expt 2G	expt 3G	MD at 66.0 Å
V_L	1203	1203**	1203**	1204
V_{HL}	289	289**	289**	288
R_{CG}	0.52	(0.52) 0.50*	(0.52) 0.50*	0.51
R_{PG1}	0.16	N/A	(0.16) 0.17*	0.16
r	1.86	(1.86) 1.78*	(1.86) 1.82*	1.80
r_{12}	0.71	(0.71) 0.71*	(0.71) 0.67*	0.64
D_B	38.5	36.3	36.5	36.7
D_{HH}	37.7	37.3	37.4	36.4
$2D_C$	29.1	27.6	27.7	27.9
D_{H1}	4.30	4.87	4.86	4.25
A	62.9**	66.3	66.0	66.0**
z_{CG}	15.9	14.6	14.4	15.2
σ_{CG}	2.82	2.62	2.48	2.66
z_{PG1}	19.3	19.3	18.9	18.6
σ_{PG1}	2.73	2.90	2.45	2.57
z_{PG2}	19.7	N/A	21.1	18.9
σ_{PG2}	3.36	N/A	3.3**	3.21
z_{CH}	7.8	7.8**	7.8**	7.5
σ_{CH}	3.26	3.2**	3.2**	3.17
σ_{HC}	2.87	(2.44) 2.64*	(2.44) 2.63*	2.65
σ_{CH3}	3.56	3.6**	3.71	3.61

[a] The first column shows results of the MD simulation performed at an A of 62.9 Å^2, while the second and third columns tabulate the results obtained from experimental data using the 2G and 3G SDP models, respectively. The last column displays results of the final simulation performed at A = 66.0 Å^2. All parameters are shown in their appropriate units for length (Å), area (Å^2), and volume (Å^3), with estimated uncertainties of ±2%. The double asterisks (**) denote hard constrained parameters, while single asterisks (*) denote "soft" constrained parameters. Target values are shown in parentheses.

parameters place strict limits on parameter space. Nevertheless, the counting statistics of these experimental data, in addition to their limited q-ranges, do not allow for all structural features to be described fully. For example, in previous studies involving PC headgroup lipids,[7] the widths of the three headgroup Gaussians proved to be the most insensitive parameters. In the present study, this turns out to be especially true in the case of the PG2 component. Unconstraining this parameter results not only in a very narrow peak that is physically unrealistic for liquid crystalline bilayers but also gives rise to strong oscillations in the high q-range where no experimental data are available. It should be noted, however, that the width of the PG2 Gaussian has only a minor effect on χ^2, and a 1 Å change to its width alters the area per lipid by only 0.3 Å^2. This change is well within the estimated uncertainties for our lipid area, and as such we fixed the value of this parameter (i.e., width of the PG2 Gaussian) to that obtained from the simulation.

Another input parameter required for the SDP analysis is volumetric information, which we also estimate from simulations utilizing the SIMtoEXP software.[19] The values for total lipid volume (V_L), headgroup volume (V_{HL}), as well as the ratios of partial volumes $r = V_{CH3}/V_{CH2}$, $r_{12} = V_{CH}/V_{CH2}$, $R_{CG} = V_{CG}/V_{HL}$, and $R_{PG1} = V_{PG1}/V_{HL}$ are restricted to those values obtained from the SIMtoEXP software (see Table 1). It is worth noting the reasonable agreement between the total lipid volume obtained from our simulation (V_L = 1203 Å^3) and the one obtained experimentally ($V_L \sim$ 1208 Å^3, Tristram-Nagle, personal communication). It needs to be stressed, however, that the uncertainty in the total lipid volume is the biggest source of error to the area per lipid value. This is a direct result of A being equal to V_L/D_B, where bilayer thickness, D_B, is one of the primary pieces of information that we obtain from the experimental scattering form factors.

Finally, and in agreement with our previous notion, is that calculated lipid volumes are similar regardless of the headgroup parsing used [i.e., two (2G) or three Gaussians (3G)] to interpret the MD simulation data (not shown). This also holds true for most of the structural parameters obtained while fitting the two SDP models to experimental data. However, the width of the CH_3 component was found to be erratic when using the 2G SDP model to fit the data, and as such it had to be constrained. In addition, the results tabulated in the third column of Table 1 (i.e., expt - 3G), show that the distributions of the two PG components (i.e., z_{PG1} and z_{PG2}) are shifted by more than 2 Å. This implies the nonparallel orientation of the PG headgroup with respect to the bilayer surface, further justifying the use of the 3G SDP model to analyze the experimental data.

Fits to the X-ray form factors using the 3G SDP model are shown in Figure 4 and seem to be in very good agreement over the entire q-range (q < 0.8 Å^{-1}) - although the data are statistically "noisy" above q = 0.6 Å^{-1}. Such high-quality data typically result in high-resolution electron density profiles revealing detailed bilayer structural features. In contrast, the figure with the neutron scattering data shows form factors extending only up to q < 0.3 Å^{-1} with statistical noise increasing considerably beyond q = 0.2 Å^{-1}—data typical from SANS measurements of liquid crystalline bilayers in solution. Despite their lesser quality, these low-q-region neutron data contain robust information regarding the water distribution and the bilayer thickness. As in previous studies, we implemented the concept of the Gibbs dividing surface[34] to determine the relevant structural parameters.

One important structural parameter, especially when considering the hydrophobic matching of lipids and proteins, is the hydrocarbon chain thickness, D_C—the SDP model defines D_C at the center of the error function, i.e., the hydrocarbon chain distribution (see Figure 4). Another important parameter is the total bilayer thickness, D_B, which we define as the Gibbs dividing surface for the water region (i.e., $D_B/2$). As mentioned and extensively discussed in a previous publication,[7] D_B is robustly determined by neutron scattering and leads to the accurate determination of A (i.e., $A = 2V_L/D_B$). On the other hand, X-ray scattering is highly sensitive to the electron-dense lipid headgroups, providing the head-to-head distance, D_{HH}. All four parameters are crucial to describing the overall bilayer structure and are shown in Table 1 in addition to other SDP-derived parameters.

The SDP analysis results presented in Figure 4 provide the detailed structure of POPG bilayers as determined from experimental data. Although the structural values are obtained using a model-based approach, their validity is suggested by their reproducibility and the robustness of the model. The SDP model fitted simultaneously to SAXS and various contrast SANS data yields an area per lipid for liquid crystalline POPG bilayers of 66.0 ± 1.3 Å^2, assuming the simulated value of V_L = 1203 Å^3. Below, we reconfirm POPG's area per lipid in the final comparison of experimental and MD simulated data using the model-free approach.

dx.doi.org/10.1021/jp208920h |J. Phys. Chem. B 2012, 116, 232–239

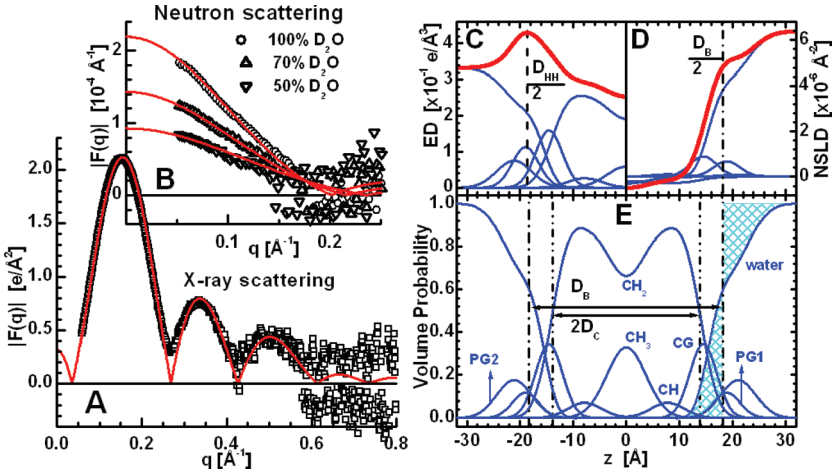

Figure 4. POPG bilayer (30 °C) structure determination through the simultaneous analysis of X-ray and neutron scattering data. Graphs on the left show the experimental X-ray (A) and the contrast varied neutron (B) scattering form factors (points), together with best fits to the data (solid lines). The SDP model of a bilayer in real space is shown on the right, where the top panels show electron densities (C) and neutron scattering length densities (D) of the various components making up the bilayer, including the total scattering densities (thick lines). Panel (E) shows volume probability distributions, where the total probability is equal to 1 at each point along the bilayer. The definition of the Gibb's dividing surface is graphically shown (E) to be a point along the *z*-axis where the integrated water distribution areas (hatched) are equal, i.e., effectively the interface between the lipid bilayer and water (i.e., $D_B/2$).

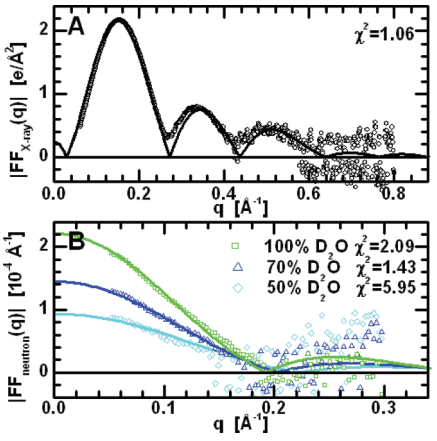

Figure 5. X-ray (A) and different deuteration neutron scattering form factors (B) calculated from MD simulation data performed at $A = 66.0$ Å^2 (solid lines) and compared to experimental data (points). Experimental data points are scaled according to eq 3 and χ^2 values are calculated according to eq 4.

SIMtoEXP Comparison. MD simulations are performed at the fixed area per lipid of 66.0 Å^2, and the results are directly compared to the experimental data (i.e., form factors). Shown in Figure 5 are the various form factors from X-ray, neutron, and MD simulations. From the data presented in the figure, it is clear that there is very good agreement (i.e., low χ^2 values) between the simulated form factors and those obtained experimentally. A noted exception is the 50% D_2O neutron scattering data, whose χ^2 value is slightly higher than that from the initial simulation (see Figure 1). We rationalize this on the basis of large experimental errors present in the 50% D_2O data, making the comparison of this data to the simulated data rather insensitive to changes in the simulation.

The good agreement between simulated and experimental data (i.e., model-free analysis) gives us confidence in the POPG area per lipid value as determined using the SDP model-based approach. In addition to A and D_B whose determination greatly benefits from the strong neutron scattering contrast between the lipid bilayer and 100% D_2O, the MD simulation provides additional, and much valued structural information using the suite of routines that are part of the SIMtoEXP software[19] (see Figure 6). For example, SIMtoEXP incorporates a procedure for extracting component volumes from simulations according to ref 35. The calculated values (shown in the bottom-right panel of SIMtoEXP, Figure 6) agree closely with those values extracted from the initial simulation, suggesting that both simulations are well equilibrated and do not alter, to any great extent, the bilayer's internal structure by changing the "fixed" area per lipid. This is also consistent with component distributions resembling the same functional forms (i.e., Gaussians and the error function), thus providing further validation of the SDP model.

The results obtained by using the SIMtoEXP software are listed in Table 1. As mentioned, most of the structural parameters do not exceed the estimated uncertainties when comparing the two simulations. However, it is not surprising to find that the results of the 66.0 Å^2 lipid area simulation are compressed in the lateral direction (i.e., bilayer thickness). This behavior is easily understood as A relates inversely to bilayer thickness (i.e., $D_B = 2V_L/A$); note that the volumes in both simulations are very similar. The increased area per lipid and the consequent thinning of the bilayer also shows up in reciprocal space (i.e., the form factor). The most pronounced effect is the shift to higher q of the first minimum in the 100% D_2O neutron scattering simulation results (compare Figures 1B and 5B) that translates into D_B decreasing by almost 2 Å. In the case of the X-ray data, the shifts of the form factor minima are less pronounced as they are mostly affected by changes in D_{HH} and D_C. It has previously been suggested[7] that D_{HH} and D_C can be altered with little impact to the total electron density profile, and thus scattering form factors, assuming that D_{H1} also changes ($D_{H1} = D_{HH}/2 - D_C$). D_{H1} values have generally been obtained from gel-phase lipid bilayers and/or simulation results, but their validity has been questioned. It has also been discussed that D_{H1} values are not lipid independent[7]

dx.doi.org/10.1021/jp208920h |*J. Phys. Chem. B* 2012, 116, 232–239

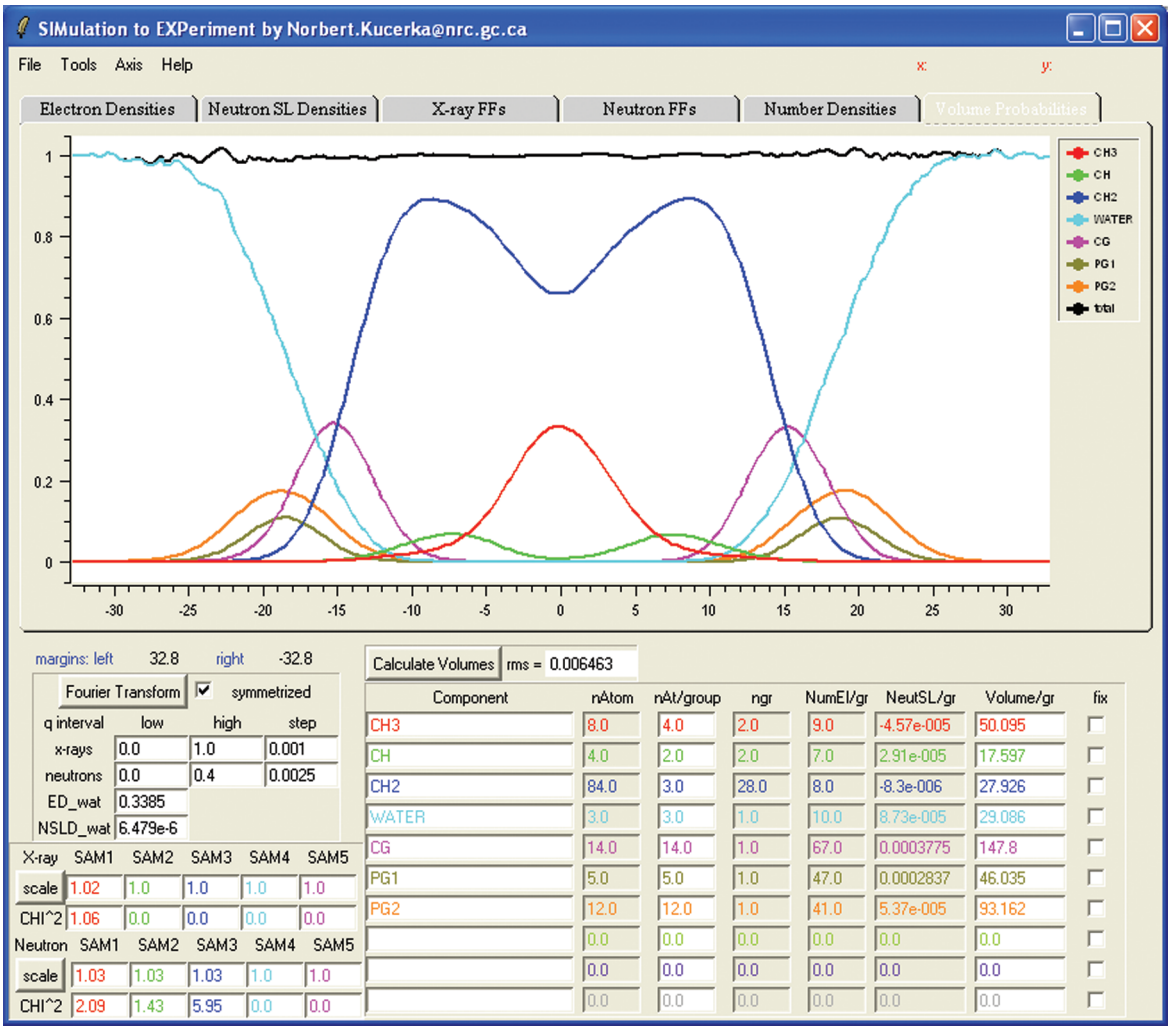

Figure 6. A snapshot of the SIMtoEXP software[19] in which the volume probability distributions of the components (colors) and their sum (black) are graphically displayed for the POPG bilayer simulated at A = 66.0 Å^2. The bottom left part of the graphical user interface (GUI) shows results of direct comparisons between simulated and experimental data, while the lower right part shows the results from volumetric analysis (given in Å^3). In the case of this example, the tabs at the top of the GUI allow the user to visualize the results for electron density, neutron scattering length density, X-ray form factors, neutron form factors, number density, and volume probability.

and that using standalone X-ray data allows for ambiguity in the values of strongly coupled parameters such as A and D_{H1}. On the other hand, this ambiguity is removed by the inclusion of neutron data.[36] In the case of POPG bilayers, D_{H1} = 4.86 Å was obtained in the SDP analysis utilizing neutron scattering data instead of simulated data.

The comparison of structural parameters obtained from the SDP analysis (third column of Table 1) and those obtained from MD simulation performed at an area per lipid of 66.0 Å^2 (last column of Table 1) shows good agreement (within estimated uncertainties) for most parameters. For example, the close agreement in the case of D_B and $2D_C$ reveals the robustness between experimental and simulated results. On the other hand, parameters relating to headgroup structure display some non-negligible differences. The difference of 1 Å in D_{HH} is compensated by changes in D_{H1}, consistent with the above discussion and the somewhat different positions of the headgroup components. The largest difference is observed in the case of the PG2 component whose position differs by up to 2.2 Å, emphasizing the biggest discrepancy between experimental and simulated results. While the simulation suggests that the orientation of the PG1−PG2 vector is parallel to the bilayer surface, experimental results indicate that it is tilted by almost 20° from a parallel orientation. Although it is not clear as to how one goes about to reconcile these differences, it has been pointed out, both by us and others,[37] that the structural parameters for the lipid headgroup and the water, along with their simulation interaction parameters, require further refinement.

The need for the further refinement of the force fields utilized in MD simulations is also supported when comparing our results to MD simulations by Zhao et al.[5] They reported an area per POPG of 53 Å^2, a value about 19% smaller than what they obtained for POPC. The authors attribute this unusually small area per lipid to the PG headgroups forming ionic bridges with Na^+ ions. However, it is clear from our experimental results that, compared to POPC,[4] POPG has an area per lipid that is 3% greater. The Zhao et al. result is most likely an artifact of poor parametrization in their MD simulation. To avoid similar erroneous conclusions, it is crucial that the various employed MD force

dx.doi.org/10.1021/jp208920h |J. Phys. Chem. B 2012, 116, 232–239

fields replicate experimental data.[38] Although this work does not directly contribute to force field development, it does provide invaluable experimental information that can be utilized by simulators in the development of such force fields.

CONCLUSIONS

We combined MD simulations and experiment (both SANS and SAXS) to determine the precise structure of liquid crystalline POPG bilayers. Experiment and simulation were utilized in a manner such that the simulation results were used to guide the development of a lipid bilayer scattering density profile that was suitable for the analysis of experimental data. A model-based analysis of the experimental data resulted in an area per lipid of 66.0 Å^2, a value which was then used in a fixed-area simulation. In the final step of this data analysis process, the direct comparison of simulated to experimental data provided the model-free structure of POPG bilayers. In the near future, we will apply the now developed SDP model for POPG bilayers to determine the structure of other commonly used liquid crystalline PG bilayers.

AUTHOR INFORMATION

Corresponding Author

*Phone: 613-584-4718, x44195. Fax: 613-584-4040. E-mail: Norbert.Kucerka@nrc-cnrc.gc.ca (N.K.); KatsarasJ@ornl.gov (J.K.).

ACKNOWLEDGMENT

This work acknowledges facilities support from the National Institute of Standards and Technology (NIST) supported in part by the National Science Foundation under agreement No. DMR-0944772, and the Cornell High Energy Synchrotron Source (CHESS) supported by the National Science Foundation and the National Institutes of Health/National Institute of General Medical Sciences under National Science Foundation award DMR-0225180. J.K. is supported by Oak Ridge National Laboratory's (ORNL) Laboratory Directed Research and Development (LDRD) and Program Development programs. This work was made possible by the facilities of the Shared Hierarchical Academic Research Computing Network (SHARCNET www.sharcnet.ca) and Compute/Calcul Canada.

REFERENCES

(1) Zasloff, M. *Nature* **2002**, *415*, 389–395.
(2) Vivcharuk, V.; Tomberli, B.; Tolokh, I. S.; Gray, C. G. *Phys. Rev. E* **2008**, *77*, 031913.
(3) Tolokh, I. S.; Vivcharuk, V.; Tomberli, B.; Gray, C. G. *Phys. Rev. E* **2009**, *80*, 031911.
(4) Kučerka, N.; Nieh, M. P.; Katsaras, J. *Biochim. Biophys. Acta* **2011**, *1808*, 2761–2771.
(5) Zhao, W.; Rog, T.; Gurtovenko, A. A.; Vattulainen, I.; Karttunen, M. *Biophys. J.* **2007**, *92*, 1114–1124.
(6) Pabst, G.; Kučerka, N.; Nieh, M. P.; Rheinstädter, M. C.; Katsaras, J. *Chem. Phys. Lipids* **2010**, *163*, 460–479.
(7) Kučerka, N.; Nagle, J. F.; Sachs, J. N.; Feller, S. E.; Pencer, J.; Jackson, A.; Katsaras, J. *Biophys. J.* **2008**, *95*, 2356–2367.
(8) Wiener, M. C.; White, S. H. *Biophys. J.* **1991**, *59*, 174–185.
(9) Feller, S. E.; Pastor, R. W. *J. Chem. Phys.* **1999**, *111*, 1281–1287.
(10) Kučerka, N.; Tristram-Nagle, S.; Nagle, J. F. *Biophys. J.* **2006**, *90*, L83–L85.
(11) Feller, S. E.; MacKerell, A. D. *J. Phys. Chem. B* **2000**, *104*, 7510–7515.
(12) Klauda, J. B.; Brooks, B. R.; MacKerell, A. D., Jr.; Venable, R. M.; Pastor, R. W. *J. Phys. Chem. B* **2005**, *109*, 5300–5311.
(13) Sonne, J.; Jensen, M. O.; Hansen, F. Y.; Hemmingsen, L.; Peters, G. H. *Biophys. J.* **2007**, *92*, 4157–4167.
(14) Anézo, C.; de Vries, A. H.; Höltje, H. D.; Tieleman, D. P.; Marrink, S. J. *J. Phys. Chem. B* **2003**, *107*, 9424–9433.
(15) Sapay, N.; Tieleman, D. P. *J. Comput. Chem.* **2011**, *32*, 1400–1410.
(16) Kučerka, N.; Gallová, J.; Uhríková, D.; Balgavý, P.; Bulacu, M.; Marrink, S. J.; Katsaras, J. *Biophys. J.* **2009**, *97*, 1926–1932.
(17) Klauda, J. B.; Kučerka, N.; Brooks, B. R.; Pastor, R. W.; Nagle, J. F. *Biophys. J.* **2006**, *90*, 2796–2807.
(18) Braun, A. R.; Sachs, J. N. *Annu. Rep. Comput. Chem.* **2011**, *7*, 125–150.
(19) Kučerka, N.; Katsaras, J.; Nagle, J. F. *J. Membr. Biol.* **2010**, *235*, 43–50.
(20) Avanti Polar Lipids. 2011, http://www.avantilipids.com/.
(21) Kučerka, N.; Pencer, J.; Sachs, J. N.; Nagle, J. F.; Katsaras, J. *Langmuir* **2007**, *23*, 1292–1299.
(22) Kučerka, N.; Liu, Y.; Chu, N.; Petrache, H. I.; Tristram-Nagle, S.; Nagle, J. F. *Biophys. J.* **2005**, *88*, 2626–2637.
(23) Glinka, C. J.; Barker, J. G.; Hammouda, B.; Krueger, S.; Moyer, J. J.; Orts, W. J. *J. Appl. Crystallogr.* **1998**, *31*, 430–445.
(24) Kline, S. R. *J. Appl. Crystallogr.* **2006**, *39*, 895–900.
(25) Phillips, J. C.; Braun, R.; Wang, W.; Gumbart, J.; Tajkhorshid, E.; Villa, E.; Chipot, C.; Skeel, R. D.; Kale, L.; Schulten, K. *J. Comput. Chem.* **2005**, *26*, 1781–1802.
(26) MacKerell, A. D., Jr.; Banavali, N.; Foloppe, N. *Biopolymers* **2000**, *56*, 257–265.
(27) Noy, A.; Soteras, I.; Luque, F. J.; Orozco, M. *Phys. Chem. Chem. Phys.* **2009**, *11*, 10596–10607.
(28) Timko, J.; Bucher, D.; Kuyucak, S. *J. Chem. Phys.* **2010**, *132*, 114510.
(29) Jo, S.; Kim, T.; Iyer, V. G.; Im, W. *J. Comput. Chem.* **2008**, *29*, 1859–1865.
(30) Humphrey, W.; Dalke, A.; Schulten, K. *J. Mol. Graph.* **1996**, *14*, 33–38.
(31) Benz, R. W.; Castro-Roman, F.; Tobias, D. J.; White, S. H. *Biophys. J.* **2005**, *88*, 805–817.
(32) Kučerka, N.; Perlmutter, J. D.; Pan, J.; Tristram-Nagle, S.; Katsaras, J.; Sachs, J. N. *Biophys. J.* **2008**, *95*, 2792–2805.
(33) Wiener, M. C.; Suter, R. M.; Nagle, J. F. *Biophys. J.* **1989**, *55*, 315–325.
(34) Nagle, J. F.; Tristram-Nagle, S. *Biochim. Biophys. Acta* **2000**, *1469*, 159–195.
(35) Petrache, H. I.; Feller, S. E.; Nagle, J. F. *Biophys. J.* **1997**, *72*, 2237–2242.
(36) Tristram-Nagle, S.; Kim, D. J.; Akhunzada, N.; Kučerka, N.; Mathai, J. C.; Katsaras, J.; Zeidel, M.; Nagle, J. F. *Chem. Phys. Lipids* **2010**, *163*, 630–637.
(37) Castro-Roman, F.; Benz, R. W.; White, S. H.; Tobias, D. J. *J. Phys. Chem. B* **2006**, *110*, 24157–24164.
(38) Klauda, J. B.; Venable, R. M.; Freites, J. A.; O'Connor, J. W.; Tobias, D. J.; Mondragon-Ramirez, C.; Vorobyov, I.; MacKerell, A. D., Jr.; Pastor, R. W. *J. Phys. Chem. B* **2010**, *114*, 7830–7843.